Surface Roughness Parameters Evaluation in Machining GFRP Composites by PCD Tool using Digital Image Processing

P. M. M. S. SARMA*
Sri Sairam Engineering College, Mechanical Engineering, India

L. KARUNAMOORTHY
Anna University, Mechanical Engineering, India

K. PALANIKUMAR
Sathyabama University, Mechanical & Production Engineering, India

ABSTRACT: Glass fiber reinforced polymer (GFRP) composites find diverse applications in many fields. Their usage in modern automated manufacturing sector demand high quality components and high finish surfaces. As such the present paper makes a study of the surface roughness of the machined surfaces of GFRP composites at different cutting conditions. The GFRP pipes are turned in lathe using Poly-Crystalline Diamond (PCD) tool. During machining, the machined surface images are captured using a Charge Coupled Device (CCD) camera. For all the images average grey scale value (Ga) are calculated. The average grey scale values and surface roughness (Ra) values are correlated and a relation is obtained between them. Also a second order quadratic model is developed for predicting surface roughness in machining of GFRP composites. The results indicate that the developed model can be used to predict the surface roughness of machined GFRP composites. The grey scale values obtained are in good correlation with the surface roughness values measured. The effect of cutting speed, feed, depth of cut and fiber orientation angle on surface roughness is studied and found that feed affects surface roughness, followed by cutting speed and fiber orientation angle. Depth of cut is found to have no effect on surface roughness of machined GFRP composites.

KEY WORDS: GFRP composites, PCD tool, CCD camera, average grey scale value (Ga), average surface roughness (Ra).

INTRODUCTION

GLASS FIBER REINFORCED polymer (GFRP) composites have been widely used in the aircraft industry and many other industries. The applications demand high quality components with respect to dimensional accuracy, form, and surface finish. The measurement of surface finish with high accuracy has become highly important. Until now the stylus probe instruments have been used for measuring the surface finish of a

*Author to whom correspondence should be addressed. E-mail: pmms_sarma@rediffmail.com
Figures 1, 4 and 7–15 appear in color online: http://jrp.sagepub.com

0731-6844/09/13 1567–19 $10.00/0 DOI: 10.1177/0731684408089858

machined surface that used the vertical displacement of a diamond tipped probe. Though the process is accurate and accepted widely by all users, the method is not suitable for high volume applications as it is time consuming and cumbersome. Also, it requires direct physical contact with the work piece surface under investigation and the resolution of the instrument depends on the diameter of the probe used.

With increasing demand of industrial automation in manufacturing, machine vision plays an important role in quality inspection and process monitoring. The major advantage of using machine vision for measuring surface finish is that it is a non-contact method of inspecting the components and also the fastest method compared to any other contact methods of inspection.

Ramulu et al. [1] carried out a study on machining of polymer composites and concluded that higher cutting speeds give better surface finish. Takeyama and Lijama [2] studied the surface roughness on machining of GFRP composites. According to them, higher cutting speed produce more damages on the machined surface. This is attributed to higher cutting temperature, which results in local softening of work material. They also studied the machinability of FRP composites using the ultrasonic machining technique. According to Konig [3], measurement of surface roughness in FRP is less dependable, compared to that in metals, because protruding fiber tips may lead to incorrect results. Additional errors may result from the hooking of the fibers to the stylus. Palanikumar [4] studied the effect of cutting parameters on surface roughness on the machining of GFRP composites by poly-crystalline diamond (PCD) tool by developing a second-order model for predicting the surface roughness. Most of the studies on GFRP composite machining showed that minimizing the surface roughness is very difficult and is to be controlled [4–14]. In another study, Palanikumar et al. [15] have developed a procedure to assess and optimize the chosen factors to attain minimum surface roughness by incorporating response table and response graph, normal probability plot, interaction graphs, and analysis of variance (ANOVA) technique.

Priya and Ramamoorthy [16] estimated and analyzed the optical roughness parameters of the machined surfaces by deliberately keeping them at various angles inclined to the horizontal and capturing the images using a machine vision system. Lee and Tarng [17] established a model of surface roughness based on features of the surface image and its associated cutting operations using a self-organizing adaptive learning tool called polynomial network (PN). Kuang-Chyi Lee et al. [18] utilized an adaptive neuro fuzzy inference system (ANFIS) to establish the relationship between actual surface roughness and texture features of the surface image. Liu and Jernigan [19] considered texture feature extraction and classification in an additive noise environment. They extracted 28 features from the local power and phase spectra (taken over regions of homogeneous texture). Using a method of successive addition and deletion, subsets of features were chosen and they were evaluated according to their ability to discriminate and classify samples of natural textures corrupted by additive noise with varying signal to noise ratios.

In this article, GFRP composite pipes are machined in a conventional lathe by PCD tool. For experimentation, the central composite design is used. The images of the surfaces are captured, using a machine vision system, during machining. The average grey scale values (G_a) of the captured images are obtained through a program developed by the authors in MATLAB. The surface roughness (R_a) values are also measured conventionally. A second-order quadratic model is developed for predicting surface roughness in machining of GFRP composites by the response surface methodology approach. The experimental R_a and G_a values obtained from the images are correlated using linear regression analysis.

EXPERIMENTATION

The GFRP composite pipes with E-glass fibers and polyester resin are manufactured by the filament winding process. The specifications of the fiber and resin are presented in Table 1. The pipes are of 60 mm internal diameter with 10 mm wall thickness. The pipes are machined in an all-geared lathe and a machine vision system is attached to capture the images of the work surface while being machined. The machine vision system employed consists of a WATEC 902B ½″ CCD monochrome camera with CCIR (European Standard) output and a pixel resolution of 768×574, a 2 MB on board memory PC-VISION frame grabber, a digitizer, and a personal computer. The schematic diagram of the machine vision system used is shown in Figure 1. The GFRP pipes are turned in a BHARAT all-geared lathe of model NAGMATI-175 with a maximum speed of 1200 rpm and power of 2.25 kW. The ISO specification of the tool holder used for the turning operation is a WIDAX tool holder PC LNR 1616 K12 and the tool material used for the study is polycrystalline diamond (PCD) which is a synthetic diamond product that is produced by sintering together selected diamond particles with a metal matrix using sophisticated technology. Polycrystalline tipped

Table 1. Specifications of fiber and resin.

Fibre: E-glass – RO99 1200 P556	**Resin, polyester**
Manufacturer: Saint Gobain Vetrotex India Ltd. RO99–Multi-filament Roving 1200–Linear Density, Tex P556–Sizing reference for vetrotex	Manufacturer: Mechemco Product: Mechster: 1110W (Isopthalate resin) Thinner: Styrene

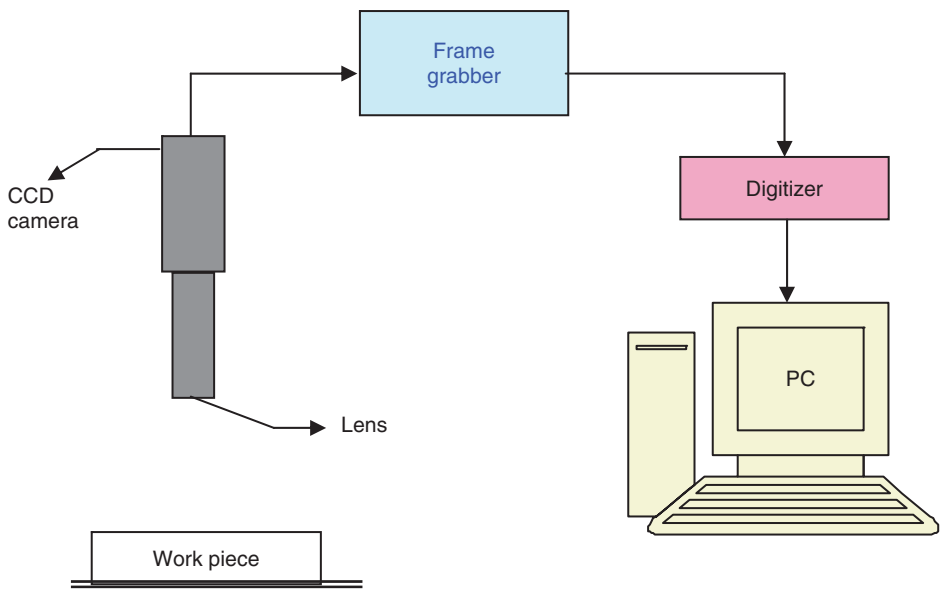

Figure 1. *Schematic diagram of machine vision system.*

Table 2. Machining parameters, their notation and their limits.

Process parameter with units	Notation	variable	Levels				
			−2	−1	0	+1	+2
Speed, m/min	V	x_1	54	82	126	194	302
Feed, mm/rev.	f	x_2	0.048	0.096	0.143	0.191	0.238
Depth of cut, mm	d	x_3	0.25	0.5	0.75	1.0	1.25
Fiber orientation angle, deg	ϕ	x_4	30	45	60	75	90

tools are exceptionally resistant to wear compared to tungsten carbide or ceramic tools. In certain applications, PCD tool life can exceed carbide cutting tool life by 50–100 times. The tool insert is PLANSEE-TIZIT of type CNMG 120408. During machining, different surface textures are obtained by varying the machining parameters. The experiments are conducted as per the central composite design (CCD) in design of experiments [20].

In the current investigation the number of variables considered for the response surface modeling are, four x variables, viz., x_1, x_2, x_3, and x_4 and the number of experiments conducted are 31. The alpha value selected as per central composite design is 2. The plan consists of sixteen (2^4) factorial design, plus eight star points and seven center points. The independently controllable process parameters identified are: cutting speed (V) in m/min, feed (f) in mm/rev, depth of cut (d) in mm, and fiber orientation angle of the work piece (ϕ), in degrees. The selected process parameters, their notations, and their limits are given in Table 2. The process parameter values and observed response, i.e., average surface roughness (R_a) values for all the 31 experiments are listed in Table 3.

For each experiment the surface texture of the machined surface has been captured by the CCD camera. The images are stored in a bitmap file and later they are analyzed for their average gray scale (G_a) values with the help of a program written in MATLAB. Also the roughness (R_a) of the machined surfaces is measured conventionally using a surface roughness tester Surtronic 3^+ manufactured by Taylor and Hobson.

The surface roughness R_a is the arithmetic average of the absolute value of the heights of roughness irregularities taken from the mean value measured:

$$R_a = \frac{1}{n}\sum_{i=1}^{n} y_i \tag{1}$$

where y_i is the height of roughness irregularities from that of the mean value and n is the number of sampling data. The parameter R_a is widely used by all the researchers and industrial users.

In the case of machine vision, average gray scale value G_a is used to estimate surface roughness. G_a is the arithmetic average of gray level intensity values and is expressed as:

$$G_a = \frac{1}{n}\sum_{i=1}^{n} g_i \tag{2}$$

Table 3. Experimental results.

	Coded variables				Uncoded variables				Surface roughness, R_a μm			
S.No.	x_1	x_2	x_3	x_4	*V* m/min	*f* mm/rev	*d* mm	ϕ°	1	2	3	Avg
1	−1	−1	−1	−1	82	0.096	0.5	45	2.454	2.306	2.632	2.464
2	1	−1	−1	−1	194	0.096	0.5	45	2.165	2.056	2.457	2.226
3	−1	1	−1	−1	82	0.191	0.5	45	2.754	3.092	3.541	3.129
4	1	1	−1	−1	194	0.191	0.5	45	2.753	2.895	3.145	2.931
5	−1	−1	1	−1	82	0.096	1.0	45	2.423	2.525	2.189	2.379
6	1	−1	1	−1	194	0.096	1.0	45	2.197	1.998	2.384	2.193
7	−1	1	1	−1	82	0.191	1.0	45	3.002	3.305	3.002	3.103
8	1	1	1	−1	194	0.191	1.0	45	2.765	2.931	3.148	2.948
9	−1	−1	−1	1	82	0.096	0.5	75	2.606	2.892	2.464	2.654
10	1	−1	−1	1	194	0.096	0.5	75	2.339	2.164	2.532	2.345
11	−1	1	−1	1	82	0.191	0.5	75	3.589	3.128	3.195	3.304
12	1	1	−1	1	194	0.191	0.5	75	2.982	2.902	3.251	3.045
13	−1	−1	1	1	82	0.096	1.0	75	2.435	2.783	2.327	2.515
14	1	−1	1	1	194	0.096	1.0	75	2.091	2.220	2.496	2.269
15	−1	1	1	1	82	0.191	1.0	75	3.219	3.459	3.009	3.229
16	1	1	1	1	194	0.191	1.0	75	2.985	2.819	3.256	3.020
17	−2	0	0	0	54	0.143	0.75	60	3.275	2.885	2.861	3.007
18	2	0	0	0	302	0.143	0.75	60	1.996	2.527	2.695	2.406
19	0	−2	0	0	126	0.048	0.75	60	2.286	1.903	2.015	2.068
20	0	2	0	0	126	0.238	0.75	60	3.195	3.220	3.557	3.324
21	0	0	−2	0	126	0.143	0.25	60	2.954	3.151	2.718	2.941
22	0	0	2	0	126	0.143	1.25	60	2.963	2.614	2.925	2.834
23	0	0	0	−2	126	0.143	0.75	30	2.726	2.681	2.345	2.584
24	0	0	0	2	126	0.143	0.75	90	2.758	2.671	3.061	2.830
25	0	0	0	0	126	0.143	0.75	60	2.829	2.747	2.443	2.673
26	0	0	0	0	126	0.143	0.75	60	2.900	2.615	2.996	2.837
27	0	0	0	0	126	0.143	0.75	60	2.963	2.764	2.541	2.756
28	0	0	0	0	126	0.143	0.75	60	2.607	2.846	2.989	2.814
29	0	0	0	0	126	0.143	0.75	60	2.760	2.858	2.428	2.682
30	0	0	0	0	126	0.143	0.75	60	2.526	2.409	2.895	2.610
31	0	0	0	0	126	0.143	0.75	60	2.876	2.698	2.484	2.686

where g_i is the difference between the gray scale intensity of individual pixels in the surface image and the mean gray value of all the pixels under consideration.

SURFACE ROUGHNESS PARAMETERS

The most important requirement in roughness measurement using machine vision is to extract the roughness parameters of surfaces using images. Surface roughness parameters are extracted based on spatial frequency domain using the 2D Fourier transform. A summary of the 2D Fourier transform definition is shown in Figure 2 [21]. The Fourier transform characterizes the surface images in terms of frequency components [22]. Liu and Jernigan [19] have derived a set of 28 texture features in the spatial frequency domain. In this study, the machine vision system is employed to characterize the surface roughness of GFRP composite specimen, which is entirely different from the machined normal metal surfaces, for which the composites contain two different matrixes such as fiber and resin.

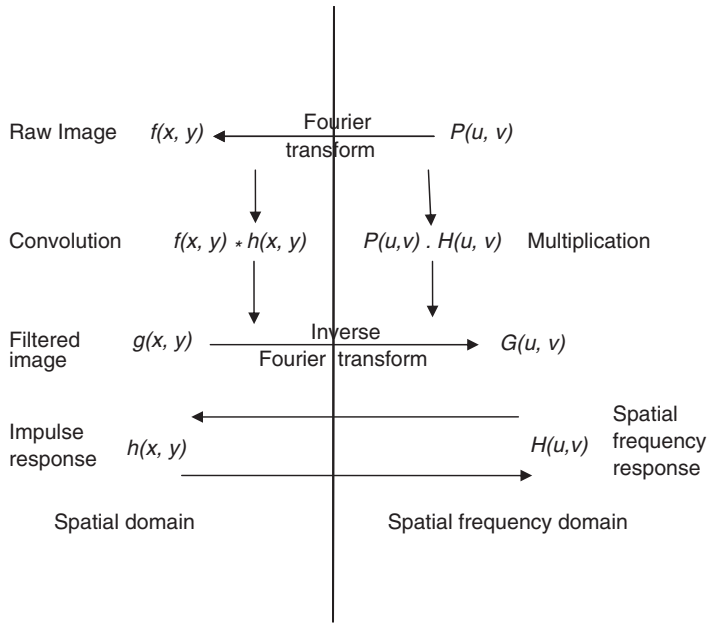

Figure 2. *Summary of two-dimensional Fourier transform definition [21].*

Let $f(x, y)$ be the gray level of a pixel at (x, y) in the original image of size $N \times N$ pixels. The discrete 2D Fourier transform [23] of $f(x, y)$ is given by:

$$F(u, v) = \frac{1}{N} \sum_{x=0}^{N-1} \sum_{y=0}^{N-1} f(x, y) \cdot \exp[-j2\pi(ux + vy)/N] \tag{3}$$

for $u,\ v = 0, 1, 2, \ldots, N-1$.

The Fourier transform is generally complex, i.e.:

$$F(u, v) = R(u, v) + jI(u, v) \tag{4}$$

where $R(u, v)$ and $I(u, v)$ are the real and imaginary components of $F(u, v)$ respectively. The Fourier spectrum $|F(u, v)|$, phase $\phi\ (u, v)$, and power spectrum $P(u, v)$ are defined by:

$$\left|F(u, v)\right| = [R^2(u, v) + I^2(u, v)]^{1/2} \tag{5}$$

$$\phi(u, v) = \tan^{-1}\left[\frac{I(u, v)}{R(u, v)}\right] \tag{6}$$

and:

$$P(u, v) = \left|F(u, v)\right|^2 = R^2(u, v) + I^2(u, v). \tag{7}$$

The specimen images of machined surfaces at different cutting speeds are shown in Figure 3 and their corresponding power spectral density graphs are shown in Figure 4. The power spectral density (PSD), describes how the power (or variance) of a time series is distributed with frequency. Mathematically, it is defined as the Fourier transform of the

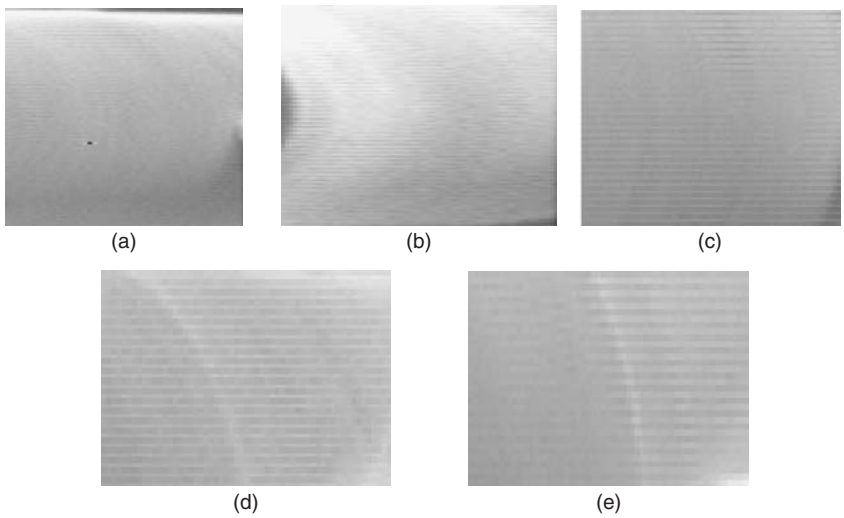

Figure 3. *Specimen images of the machined surfaces taken at (a) V = 302 m/min, (b) V = 194 m/min, (c) V = 126 m/min, (d) V = 82 m/min and (e) V = 54 m/min.*

autocorrelation sequence of the time series. An equivalent definition of PSD is the squared modulus of the Fourier transform of the time series, scaled by a proper constant term.

Let:

$$p(u, v) = \frac{P(u, v)}{\sum_{(u, v)\neq(0, 0)} P(u, v)} \tag{8}$$

be the normalized power spectrum, which has the characteristics of a probability distribution, where $P(u, v)$ is the power spectrum of the image $I(x, y)$.

RESULTS AND DISCUSSION

Surface roughness plays a predominant role in determining the machining accuracy. Though surface roughness is dependent on many factors, it is more influenced by the cutting parameters like cutting speed, feed, depth of cut, etc., for a given machine tool and work piece set-up. The mechanism of cutting in GFRP composites is due to the combination of plastic deformation, shearing and bending rupture. The occurrence of the above mechanisms depends on the flexibility, orientation, and toughness of the fibers. These constitute a surface texture on the work piece [15]. The presence of glass fibers in the polymer matrix increases hardness and strength. When GFRP composites are machined, discontinuous chips in powder form are produced which are entirely different from that produced when metals are machined. Machining of GFRP composites differ from machining of metals, because they are anisotropic and inhomogeneous material.

Figure 5 shows the SEM micrographs of the PCD tool used in this study. Figure 5(a) shows the rake face, whereas Figure 5(b) shows the flank face of the cutting tool. In these figures, it can be seen that small fiber particles are adhered to the rake and flank faces. As the machining is carried out without any coolant, the particles of the fiber got welded up to the tool face due to the temperature developed during the machining process. Due to this reason, a built-up edge formation like an aluminum machining has been observed on

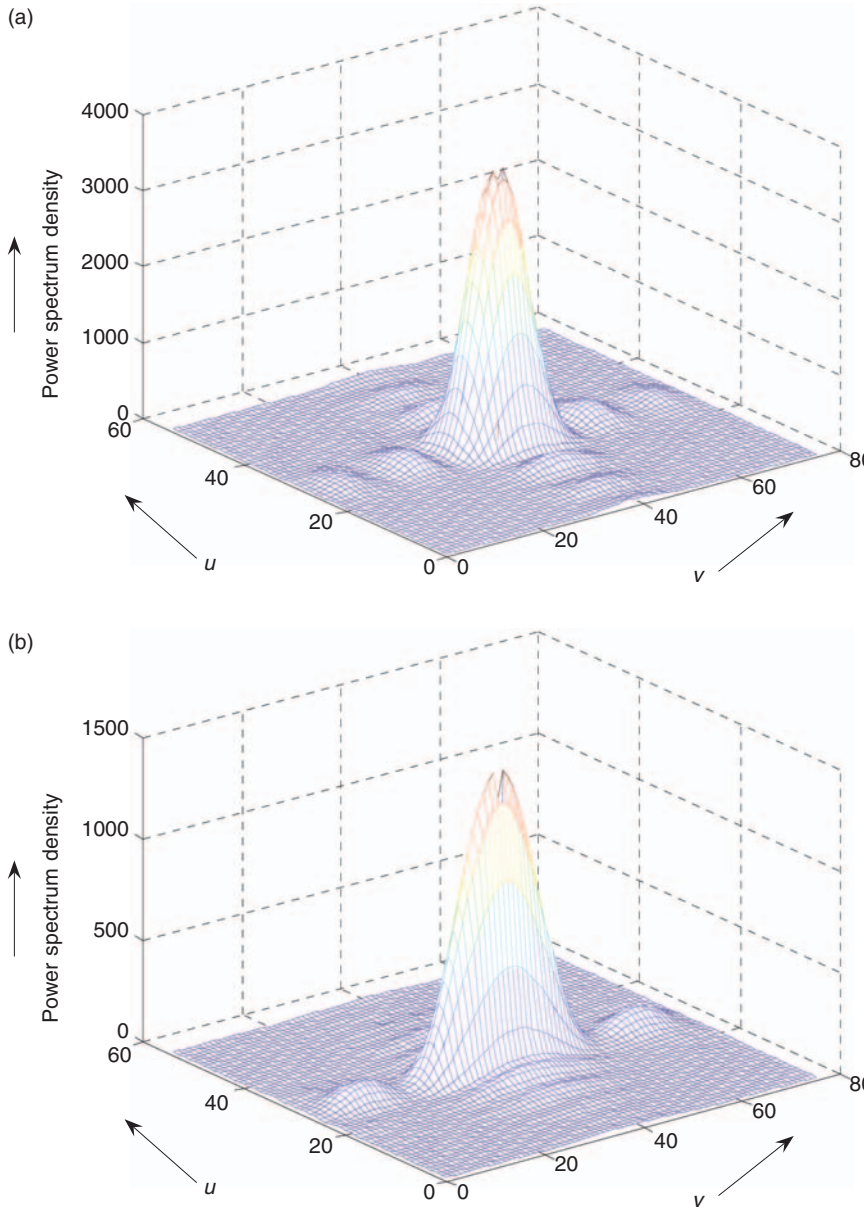

Figure 4. *Power spectrum densities of the machined surfaces at cutting speeds of (a) 54 m/min, (b) 82 m/min, (c) 126 m/min, (d) 194 m/min, and (e) 302 m/min.*

the surfaces of the tool. A small portion of flank wear pattern was also observed on the flank face. The high mechanical resistance of the fibers is the reason for excessive wear down of cutting tool and great damage to the polymeric matrix, since the fibers are taken from the matrix. In general, the cutting tool fails by gradual wear or by fracturing. The degree of tool wear influences the surface quality.

In Figure 6, SEM photographs of the machined surfaces of GFRP composites at different conditions are shown. In Figure 6(a), in the machined surface, a number of voids

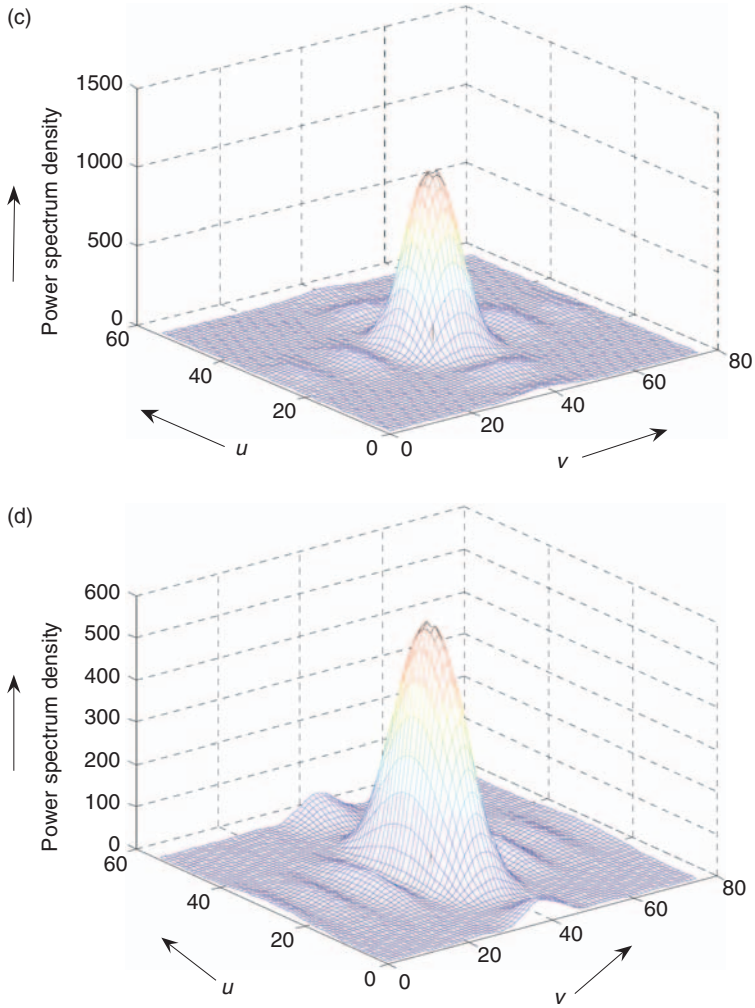

Figure 4. *Continued.*

are observed. These voids are due to the insufficient distribution of matrix and fibers in the composite materials. Figure 6(a)–(d) show the SEM images of a work piece after the cutting operation. These figures show the distribution of fibers and matrix materials after the machining operation.

The experimental values are analyzed using response surface analysis and the following relation has been established for surface roughness (R_a) in coded units and is given as:

$$\begin{aligned} R_a = {} & 2.72257 - 0.12516V + 0.34058f - 0.02725d + 0.06258\phi \\ & - 0.0065V^2 - 0.00911f^2 + 0.03876d^2 - 0.00636\phi^2 \\ & + 0.00987V^*f + 0.01303V^*d - 0.01538V^*\phi \\ & + 0.014f^*d - 0.00212f^*\phi - 0.01175d^*\phi. \end{aligned} \tag{9}$$

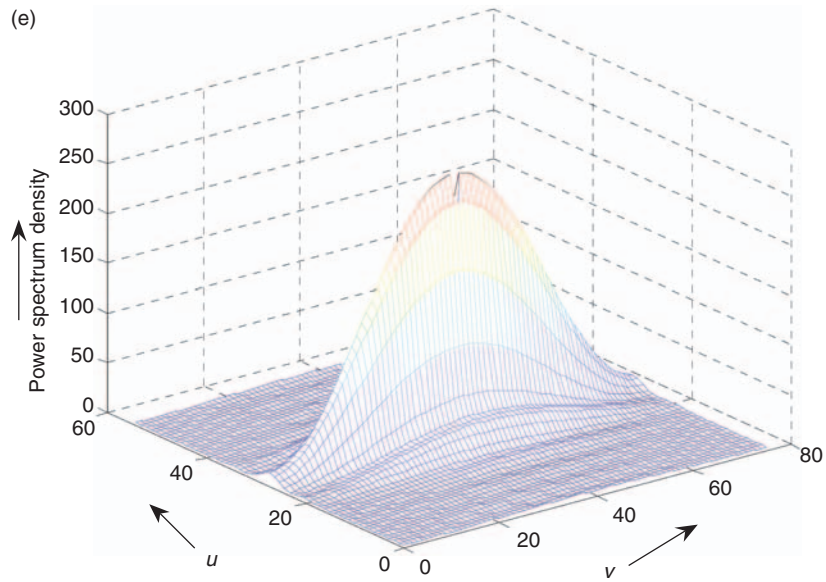

Figure 4. *Continued.*

The quantity R^2 called coefficient of determination is used to judge the adequacy of the regression model developed. $0 \leq R^2 \leq 1$. The coefficient of determination obtained for the present investigation for surface roughness is 98.3%, which shows the high correlation that exist between the experimental and predicted values.

During the experimental runs, as per the design shown in Table 3, the surface images are captured by the CCD camera for each experiment. The captured images are analyzed, and the surfaces are evaluated for their gray scale values to find the average gray scale value (G_a) and power spectrum density graphs are obtained for all 31 images. The average gray scale and surface roughness values obtained for different cutting conditions are presented in Table 4. Sample power spectrum density graphs at selected conditions are presented in Figure 4(a)–(e). From the power spectrum density graphs it is observed that with increase in cutting speed, the power spectrum density decreased which indicates improvement in surface finish.

The experimental R_a values and the G_a values obtained are correlated using linear regression analysis and the following relation is established between R_a and G_a values:

$$G_a = 5.75743 + 0.65465\ R_a. \tag{10}$$

Figures 7 and 8 show the high correlation that exists between the experimental and predicted values for R_a and G_a. The variations between the experimental results and model predicted values for both R_a and G_a are analyzed through normal probability graphs and are presented in Figure 9. The normal probability graph does not show any abnormality between the experimental results and predicted values and hence the predicted equations can be useful in prediction of surface roughness and gray scale values in machining of GFRP composites.

For analyzing the influence of machining parameters in machining of GFRP composites, the surface roughness values are calculated at different machining conditions and are plotted as shown in Figures 10–15. Figure 10 shows the variation of surface

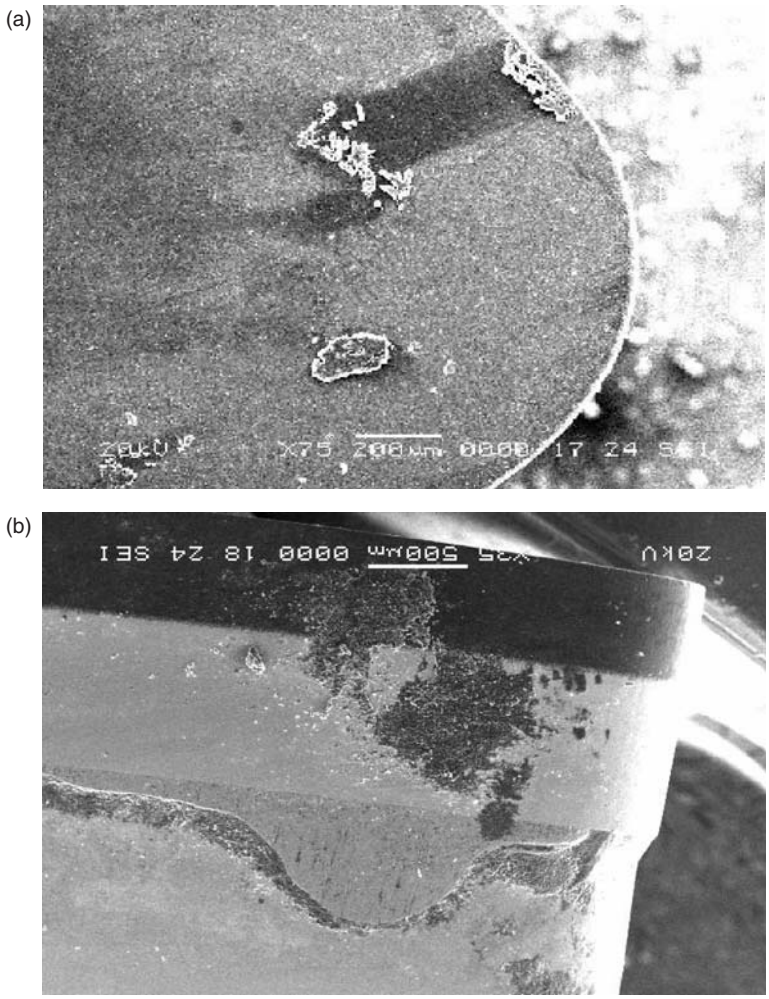

Figure 5. *SEM images of PCD tool insert (a) rake face and (b) flank face.*

roughness with cutting speed for different feeds at constant depth of cut and fiber orientation angle. It can be observed that with increase in cutting speed, the surface roughness value gets decreased which means a better finished surface can be obtained at high cutting speed. This is because at higher cutting speeds the fibers protruding out are being cut thoroughly and a fine surface is obtained. The surface roughness values are gradually increasing with increasing feed rates. In Figure 11, graphs are plotted between the cutting speed and surface roughness by varying depth of cut and keeping feed and fiber orientation angle constant. It is evident from the figure that, with the increase in depth of cut up to 1.0 mm, the surface roughness decreases and thereafter it increases gradually. Figure 12 shows the variation of cutting speed with surface roughness when fiber orientation angle values are varied keeping feed and depth of cut constant. A gradual increase is observed in surface roughness with increasing fiber orientation angle. The increase in surface roughness is more at lower cutting speeds compared to the increase of the same at higher cutting speeds.

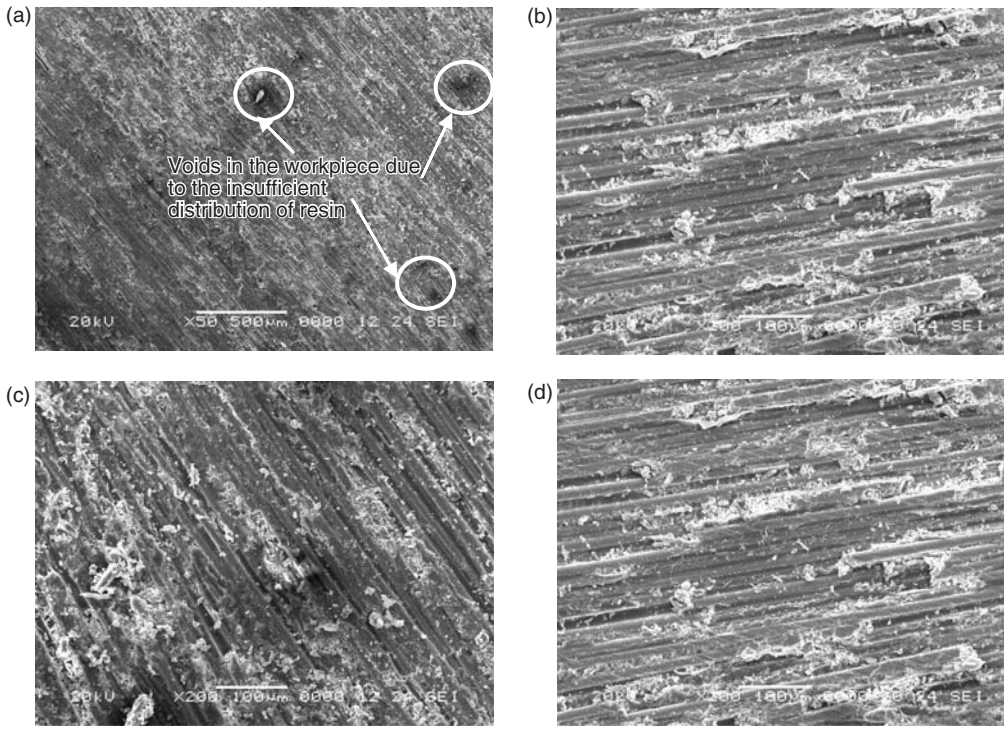

Figure 6. *(a)–(d) SEM images of the machined surface at different cutting conditions.*

Figure 13 shows the graphs plotted between feed and surface roughness for different depth of cut values keeping the cutting speed and fiber orientation angle constant. A steady increase in surface roughness is observed with increase in feed rate. When the feed is increased, some of the fibers will be eliminated from machining in each pass which will contribute to the rough surface. In Figure 14, the graphs are drawn for various values of fiber orientation angles on the plot of feed versus surface roughness keeping cutting speed and depth of cut constant. There is a little increase in surface roughness with increase in fiber orientation angle.

Figure 15 shows the graphs drawn for depth of cut and surface roughness by varying the values of fiber orientation angle keeping the cutting speed and feed constant. The surface roughness is increasing slowly with increase in fiber orientation angle. It is reducing gradually with increasing depth of cut up to a value of 1.0 mm and thereafter it is again increasing. From the above figures, it can be asserted that high cutting speed, low feed, low fiber orientation and medium depth of cut are preferred for machining of GFRP composites.

CONCLUSIONS

In this article, a second-order model has been developed for surface roughness in terms of the four machining parameters considered in the study. Also, the gray scale values of the

Table 4. Average gray scale and surface roughness values for machined surfaces obtained at different cutting conditions.

S.No.	Coded variables				Uncoded variables				Average surface roughness value R_a, μm	Average gray scale value, G_a
	x_1	x_2	x_3	x_4	V m/min	f mm/rev	d mm	ϕ°		
1	−1	−1	−1	−1	82	0.096	0.5	45	2.464	7.3986
2	1	−1	−1	−1	194	0.096	0.5	45	2.226	7.3445
3	−1	1	−1	−1	82	0.191	0.5	45	3.129	8.1735
4	1	1	−1	−1	194	0.191	0.5	45	2.931	8.1395
5	−1	−1	1	−1	82	0.096	1.0	45	2.379	7.3434
6	1	−1	1	−1	194	0.096	1.0	45	2.193	7.3095
7	−1	1	1	−1	82	0.191	1.0	45	3.103	8.1395
8	1	1	1	−1	194	0.191	1.0	45	2.948	7.9228
9	−1	−1	−1	1	82	0.096	0.5	75	2.654	7.252
10	1	−1	−1	1	194	0.096	0.5	75	2.345	7.1806
11	−1	1	−1	1	82	0.191	0.5	75	3.304	7.7216
12	1	1	−1	1	194	0.191	0.5	75	3.045	7.6772
13	−1	−1	1	1	82	0.096	1.0	75	2.515	7.1382
14	1	−1	1	1	194	0.096	1.0	75	2.269	7.0097
15	−1	1	1	1	82	0.191	1.0	75	3.229	7.6393
16	1	1	1	1	194	0.191	1.0	75	3.020	7.6382
17	−2	0	0	0	54	0.143	0.75	60	3.007	8.261
18	2	0	0	0	302	0.143	0.75	60	2.406	6.9987
19	0	−2	0	0	126	0.048	0.75	60	2.068	7.417
20	0	2	0	0	126	0.238	0.75	60	3.324	7.5811
21	0	0	−2	0	126	0.143	0.25	60	2.941	7.5704
22	0	0	2	0	126	0.143	1.25	60	2.834	7.5673
23	0	0	0	−2	126	0.143	0.75	30	2.584	7.5467
24	0	0	0	2	126	0.143	0.75	90	2.830	7.485
25	0	0	0	0	126	0.143	0.75	60	2.673	7.5314
26	0	0	0	0	126	0.143	0.75	60	2.837	7.5294
27	0	0	0	0	126	0.143	0.75	60	2.756	7.5285
28	0	0	0	0	126	0.143	0.75	60	2.814	7.5142
29	0	0	0	0	126	0.143	0.75	60	2.682	7.5074
30	0	0	0	0	126	0.143	0.75	60	2.610	7.4968
31	0	0	0	0	126	0.143	0.75	60	2.686	7.436

images of the machined surfaces are correlated with the surface roughness values and a relationship is obtained between the two by linear regression analysis. The following conclusions can be made from the study.

1. The developed second-order model for surface roughness can be used to calculate surface roughness of the machined surfaces at different cutting conditions within the chosen range.
2. A machine vision system is introduced in composites machining process, which gives good results in measuring of surface roughness without having contact with the surfaces.
3. The relationship between surface roughness R_a and gray scale value G_a can be used for measuring the surface roughness of GFRP composites.

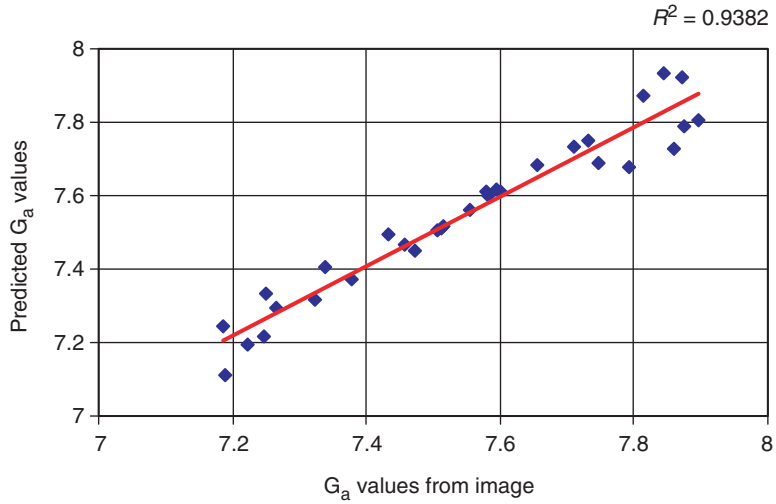

Figure 7. *Graph showing relation between image and predicted G_a values.*

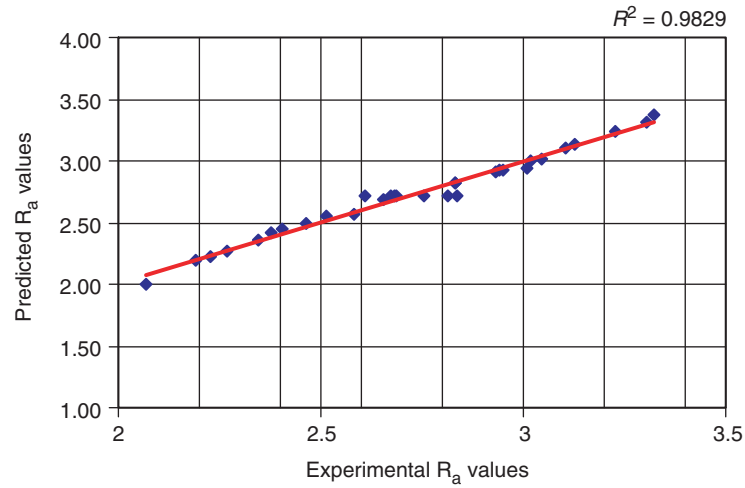

Figure 8. *Graph showing relation between experimental and predicted R_a values.*

4. It can be concluded from the power spectrum density graphs that with increase in cutting speed, the power spectrum density will decrease which means that the surface finish will improve.
5. From the results, it can be asserted that high cutting speed, low feed and low fiber orientation are preferred. Medium depth of cut is preferred for machining of GFRP composites.
6. Feed is the factor which affects surface roughness in machining of GFRP composites, followed by cutting speed and fiber orientation angle. Depth of cut shows only the limited effect in machining of GFRP composites.

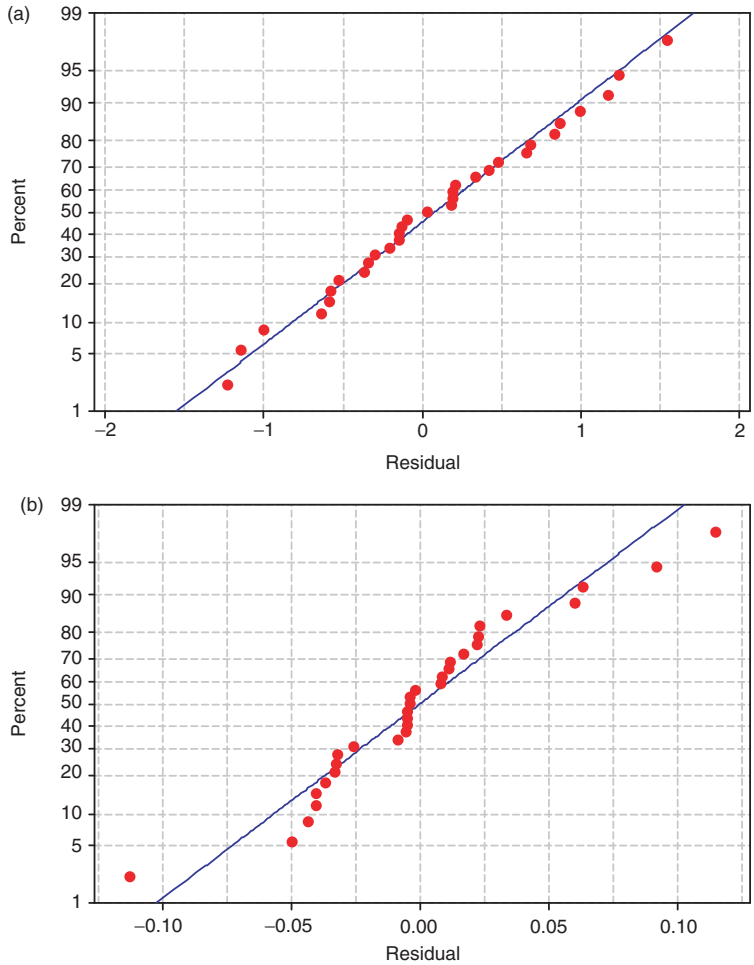

Figure 9. *(a) Normal probability plot of gray scale values, (b) Normal probability plot of surface roughness values.*

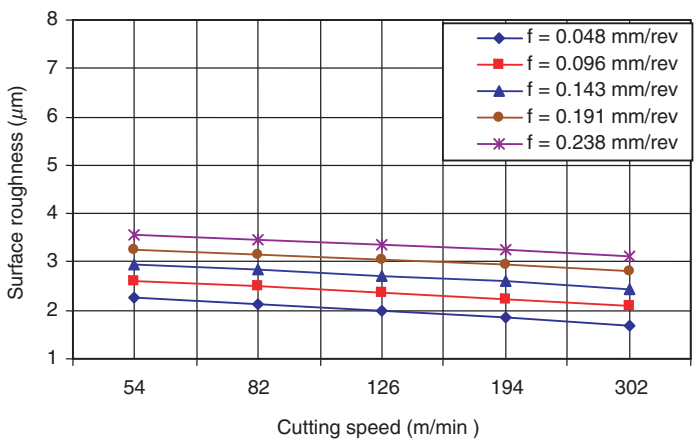

Figure 10. *Variation of surface roughness with cutting speed for different feeds at central values of depth of cut and fiber orientation angle.*

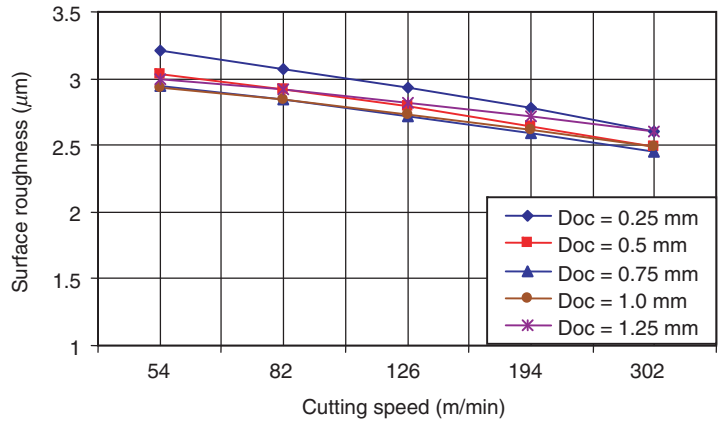

Figure 11. *Variation of surface roughness with cutting speed for different depth of cut at central values of feed and fiber orientation angle.*

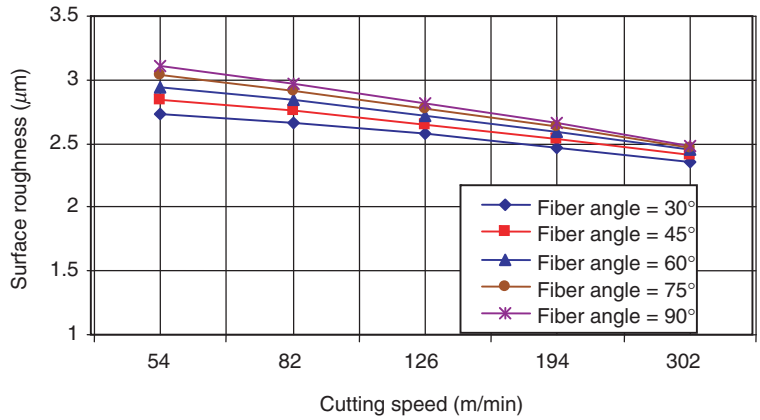

Figure 12. *Variation of surface roughness with cutting speed for different fiber orientation angles at central values of feed and depth of cut.*

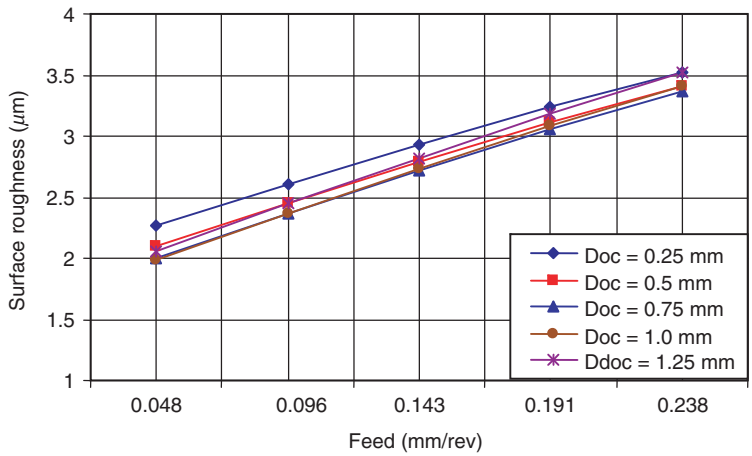

Figure 13. *Variation of surface roughness with feed for different depth of cut at central values of cutting speed and fiber orientation angle.*

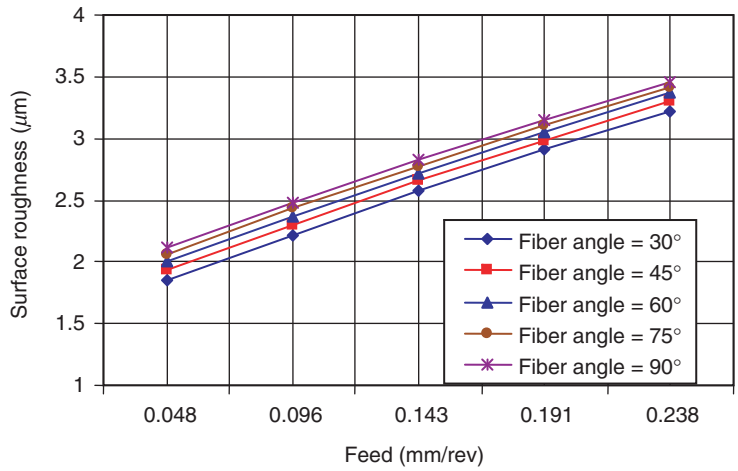

Figure 14. *Variation of surface roughness with feed for different fiber orientation angles at central values of cutting speed and depth of cut.*

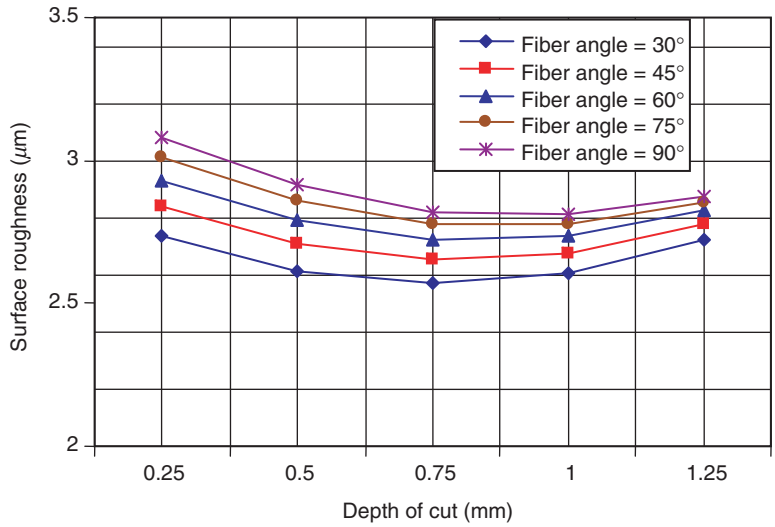

Figure 15. *Variation of surface roughness with depth of cut for different fiber orientation angles at central values of cutting speed and feed.*

NOMENCLATURE

R_a = average surface roughness value in μm
y_i = height of surface roughness from the mean value
G_a = average grey scale value
g_i = gray scale intensity of ith pixel
n = number of samples
$f(x, y)$ = gray level of the pixel at (x, y)
x, y = real variables

$F(u, v)$ = Fourier transform of $f(x, y)$
$R(u, v)$ = real component of $F(u, v)$
$I(u, v)$ = imaginary component of $F(u, v)$
u, v = frequency variables
$|F(u, v)|$ = Fourier spectrum
$\phi(u, v)$ = phase
$P(u, v)$ = power spectrum
$p(u, v)$ = normalized power spectrum
V = cutting speed in m/min
f = feed in mm/rev
d = depth of cut in mm
ϕ = fiber orientation angle in degrees

ACKNOWLEDGMENTS

The authors are highly thankful to M/S CNC Technics Private Limited, Hyderabad for giving facilities to prepare the GFRP pipes used in this work.

REFERENCES

1. Ramulu, M., Arola, D. and Colligan, K. (1994). Preliminary Investigation on the Surface Integrity of Fibre Reinforced Plastics, *Engineering Systems Design and Analysis, ASME*, **64**(2): 93–101.
2. Takeyama, H. and Lijama, N. (1988). Machinability of Glass Fibre Reinforced Plastics and Application of Ultrasonic Machining, *Annals of CIRP*, **97**(1): 93–96.
3. Konig, W., Wulf, Ch., Grab, P. and Willerscheid, H. (1985). Machining of Fiber Reinforced Plastics, *Annals of CIRP*, **34**: 537–548.
4. Palanikumar, K. (2008). Application Of Taguchi and Response Surface Methodologies for Surface Roughness in Machining Glass Fiber Reinforced Plastics by Pcd Tooling, *International Journal of Advanced Manufacturing Technology*, **36**(1–2): 19–27.
5. Sang-Ook An, Eun-Sang Lee and Sang-Lai Noh (1997). A Study on the Cutting Characteristics of Glass Fiber Reinforced Plastics with Respect to Tool Materials and Geometries, *Journal of Materials Processing Technology*, **68**: 60–67.
6. Santhanakrishnan, G., Krishnamurthy, R. and Malhotra, S. K. (1988). Machinability Characteristics of Fiber Reinforced Plastics Composites, *Journal of Mechanical Working Technology*, **17**: 95–104.
7. Paulo Davim, J. and Mata, F. (2007). New Machinability Study of Glass Fiber Reinforced Plastics Using Polycrystalline Diamond and Cemented Carbide (K15) Tools, *Materials and Design*, **28**: 1050–1054.
8. El-Sonbaty, I., Khashaba, U. A. and Machaly, T. (2004). Factors Affecting the Machinability of GFR/Epoxy Composites, *Composite Structures*, **63**: 329–338.
9. Paulo Davim, J. and Mata, F. (2004). Influence of Cutting Parameters on Surface Roughness in Turning Glass-fiber-reinforced Plastics Using Statistical Analysis, *Industrial Lubrication and Tribology*, **56**(5): 270–274.
10. Paulo Davim, J. and Mata, F. (2005). Optimisation of Surface Roughness on Turning Fiber-reinforced Plastics (FRPs) with Diamond Cutting Tools, *International Journal of Advanced Manufacturing Technology*, **26**: 319–323.
11. Isik, B. (2006). Investigation of Surface Roughness in Turning of Unidirectional GFRP Composites by Using RS Methodology and ANN, *International Journal of Advanced Manufacturing Technology*, **31**: 10–17.
12. Wang, X. M. and Zhang, L. C. (2003). An Experimental Investigation into the Orthogonal Cutting of Unidirectional Fiber Reinforced Plastics, *International Journal of Machine Tools and Manufacture*, **43**: 1015–1022.
13. Palanikumar, K., Karunamoorthy, L. and Karthikeyan, R. (2006). Parametric Optimization to Minimize the Surface Roughness on the Machining of GFRP Composites, *Journal of Materials Science Technology*, **22**(1): 66–72.
14. Lee, E. S. (2006). Precision Machining of Glass Fiber Reinforced Plastics with Respect to Tool Characteristics, *International Journal of Advanced Manufacturing Technology*, **17**: 791–798.

15. Palanikumar, K., Karunamoorthy, L. and Karthikeyan, R. (2006). Assessment of Factors Influencing Surface Roughness on the Machining of Glass Fiber-Reinforced Polymers Composites, *Materials and Design*, **27**(10): 862–871.
16. Priya, P. and Ramamoorthy, B. (2007). The Influence of Component Inclination on Surface Finish Evaluation Using Digital Image Processing, *International Journal of Machine Tools and Manufacture*, **47**(3–4): 570–579.
17. Lee, B. Y. and Tarng, Y. S. (2001). Surface Roughness Inspection by Computer Vision in Turning Operations, *International Journal of Machine Tools and Manufacture*, **41**: 1251–1263.
18. Kuang-Chyi Lee, Shinn-Jang Ho and Shinn-Ying Ho (2004). Accurate Estimation of Surface Roughness from Texture Features of the Surface Image Using an Adaptive Neuro-fuzzy Inference System, *Precision Engineering*, **29**(1): 95–100.
19. Song-Sheng Liu and Jernigan, M. E. (1990). Texture Analysis and Discrimination in Additive Noise, C*omputer Vision, Graphics and Image Processing*, **49**: 52–67.
20. Cochran, W. G. and Cox, G. M. (1963). *Experimental Designs*, Asia Publishing House, India.
21. Awcock, G. J. and Thomas, R. (1995). *Applied Image Processing*, Macmillan Press, Basingstoke, Hampshire, London.
22. Du-Ming Tsai and Jong-Jong Chen (1998). A Vision System for Surface Roughness Assessment using Neural Networks, *International Journal of Advanced Manufacturing Technology*, **14**(6): 412–422.
23. Gonzalez, R. C. and Woods, R. E. (2001). *Digital Image Processing*, Pearson Education, Asia, Addison Wesley Longman (Singapore) Pte Ltd., Indian Branch 482, Delhi, India.